JOURNAL OF BACTERIOLOGY, Aug. 1996, p. 4453–4460 Vol. 178, No. 15
0021-9193/96/$04.00+0

Involvement of the GroE Chaperonins in the Nickel-Dependent Anaerobic Biosynthesis of NiFe-Hydrogenases of *Escherichia coli*

AGNES RODRIGUE,[1] NATHALIE BATIA,[1] MATTHIAS MÜLLER,[2] OLIVIER FAYET,[3] ROBERT BÖHM,[4] MARIE-ANDREE MANDRAND-BERTHELOT,[1] AND LONG-FEI WU[1]*

Laboratoire de Génétique Moléculaire des Microorganismes et des Interactions Cellulaires, Unité Mixte de Recherche Centre National de la Recherche Scientifique 5577, INSA, 69621 Villeurbanne Cedex,[1] and Laboratoire de Microbiologie et Génétique Moléculaire, Centre National de Recherche Scientifique, 31062 Toulouse Cedex,[3] France, and Institut für Physikalische Biochemie, Universität München, D-80336 Munich,[2] and Lehrstuhl für Mikrobiologie der Universität München, D-8000 Munich,[4] Germany

Received 22 February 1996/Accepted 28 May 1996

We analyzed the involvement of chaperonins GroES and GroEL in the biosynthesis of the three hydrogenase isoenzymes, HYD1, HYD2, and HYD3, of *Escherichia coli*. These hydrogenases are NiFe-containing, membrane-bound enzymes composed of small and large subunits, each of which is proteolytically processed during biosynthesis. Total hydrogenase activity was found to be reduced by up to 60% in *groES* and *groEL* thermosensitive mutant strains. This effect was specific because it was not seen for another oligomeric, membrane-bound metalloenzyme, i.e., nitrate reductase. Analyses of the single hydrogenase isoenzymes revealed that a temperature shift during the growth of *groE* mutants led to an absence of HYD1 activity and to an accumulation of the precursor of the large subunit of HYD3, whereas only marginal effects on the processing of HYD2 and its activity were observed under these conditions. A decrease in total hydrogenase activity, together with accumulation of the precursors of the large subunits of HYD2 and HYD3, was also found to occur in a nickel uptake mutant (*nik*). The phenotype of this *nik* mutant was suppressed by supplementation of the growth medium with nickel ions. On the contrary, Ni^{2+} no longer restored hydrogenase activity and processing of the large subunit of HYD3 when the *nik* and *groE* mutations were combined in one strain. This finding suggests the involvement of these chaperonins in the biosynthesis of a functional HYD3 isoenzyme via the incorporation of nickel. In agreement with these in vivo results, we demonstrated a specific binding of GroEL to the precursor of the large subunit of HYD3 in vitro. Collectively, our results are consistent with chaperonin-dependent incorporation of nickel into the precursor of the large subunit of HYD3 as a prerequisite of its proteolytic processing and the acquisition of enzymatic activity.

The enterobacterium *Escherichia coli* synthesizes three NiFe-hydrogenase isoenzymes under anaerobic conditions (25). Hydrogenases 1 and 2 (HYD1 and HYD2, respectively) catalyze the anaerobic oxidation of hydrogen linked to the ultimate reduction of a terminal electron acceptor. These energy-conserving respiratory pathways, which enable the bacterium to use hydrogen as an energy source, allow the organism to grow on nonfermentable carbon sources such as fumarate in the presence of hydrogen. HYD3 is part of the formate hydrogenlyase complex and is responsible for formate-dependent dihydrogen evolution. This system catalyzes the oxidation of endogenously produced formate to carbon dioxide and passes the electrons so generated to protons to evolve gaseous hydrogen. The overall reaction is scalar and non-energy conserving and functions both to remove redox equivalents exchangeable with formate and to help offset acidification of the growth medium during fermentative growth. The structural genes of these hydrogenases lie in three operons, *hya*, *hyb*, and *hyc*, each of which contains four, five, and seven additional accessory genes specifically required for HYD1, HYD2, and HYD3 activities, respectively (15, 16, 22, 24). Purified HYD1 and HYD2 are heterotetramers. HYD1 consists of two identical small subunits of 35,000 Da and two identical large subunits of 64,000 Da (26), and HYD2 is composed of two identical small subunits of 35,000 Da and two identical large subunits of 61,000 Da (1). They are integral membrane proteins, and active HYD2 can be solubilized after treatment of the membrane fraction with trypsin. The large subunit of HYD3 has been purified recently (23). It is a peripheral membrane protein which is released in the soluble state when cells are broken by passage through a French press (24). All three hydrogenases contain nickel (1, 23, 25, 26).

Two forms of the large subunits of NiFe-hydrogenases from several bacteria have been observed by sodium dodecyl sulfate-polyacrylamide gel electrophoresis (SDS-PAGE). The small, faster-migrating form is recognized as the mature form, while the large, more slowly migrating form is considered its precursor. The precursor form appears in wild-type *Alcaligenes eutrophus* and *Azotobacter vinelandii* cells grown in a nickel-limited medium (4, 14). Mutations of hydrogenase structural and accessory genes can also lead to the accumulation of precursors in *E. coli* (9, 13, 17, 24) and *Alcaligenes eutrophus* (10). The processing of the hydrogenase of *Azotobacter vinelandii* (6), the selenium-containing hydrogenase of *Methanococcus voltae* (27), HYD3 of *E. coli* (23), and the periplasmic hydrogenase of *Desulfovibrio gigas* (29) results from proteolytic cleavage at a position corresponding to the highly conserved histidine residue in the motif Asp-Pro-Cys-Xaa-Xaa-Cys-Xaa-Xaa-His (DPCXXCXXH) located at the C termini of the large subunits. This motif is present in the large subunits of all known NiFe-hydrogenases and provides the ligands required for the binding of nickel (21, 29, 30). The processing of the large

* Corresponding author. Present address: Laboratoire de Chimie Bactérienne, UPR9043 CNRS, 31 Chemin Joseph Aiguier, 13402 Marseille Cedex 20, France. Phone: (33) 91 16 44 31. Fax: (33) 91 71 89 14. Electronic mail address: wu@ibsm.cnrs-mrs.fr.

subunit of HYD3 is correlated with nickel incorporation into the polypeptide chain (23).

The biosynthesis of NiFe-hydrogenases is a complex process that remains poorly understood at the molecular level. It involves the incorporation of nickel into hydrogenase apoprotein, processing of the small and large subunits, assembly of holoenzyme, and protein translocation. Some of these processes are likely to be assisted by general or specific chaperone proteins. The three major families of chaperone proteins are known as Hsp90, Hsp70, and Hsp60. This last class, also called chaperonins, is represented by the GroEL protein of *E. coli*. Horwich et al. reported that GroEL, associated with its co-chaperone GroES, assists a large set of newly translated cytoplasmic proteins to reach their native tertiary structures in *E. coli* (8). However, a more specific role in metalloprotein folding has never been documented. In this communication, we examine the effects of GroEL and GroES deficiency on the anaerobic biosynthesis of NiFe-hydrogenases in *E. coli.*

MATERIALS AND METHODS

Bacterial strains. The *groE* mutants OFB1111 (*groEL673 zjd*::Tn*10 zje*::*kan*) and JZ12 (*groES619 zje*::*kan*) are derivatives of wild-type B178 (*galE groE*$^+$) (5, 34). One of the typical phenotypes of *groE* mutant strains OFB1111 and JZ12 is that their growth is drastically reduced at 43°C. DNA sequencing analysis revealed that mutant alleles *groEL673* and *groES619* result from Gly-to-Asp substitutions at amino acid position 173 (G173D) of GroEL (34) and at amino acid position 24 (G24D) of GroES (12). Gly-173 is located in the intermediate domain of GroEL (3), and it was proposed that the mutation G173D drastically affects GroES-GroEL interaction (34). The mutation G24D lies within a mobile domain of GroES, and the mutant GroES protein is defective in its interaction with GroEL (12). Mutations *groEL673* and *groES619* result in the production of thermosensitive GroEL and GroES, respectively. HYD723 [*nikA*::MudI (*lacZ* Amp^r)] and HYD720 (Δ*nik*) are derivatives of MC4100 and are defective in a specific nickel transport system displaying the hydrogenase-minus phenotype (20, 31–33). The cellular nickel content of the *nik* mutant is less than 11% of that of the parental strain. Hydrogenase activity can be restored to the *nik* mutant by specific addition of nickel salts to the growth medium. This correlates with an increased cellular nickel content (32). To exploit this particular characteristic, isogenic *nik* and *nik groE* mutants were constructed by P1 transduction experiments (18), with HYD723 as the donor strain and B178, OFB1111, and JZ12 as receptors. Transductants were selected first for resistance to ampicillin, and the presence of the *nik* mutation was subsequently scored for by analyses of the hydrogenase activities in cells grown without and with nickel. The presence of *groE* mutations in the strains obtained, NB01 (*nik*), NB02 (*nik groES619*), and NB03 (*nik groEL673*), was analyzed by growth at 30 and 43°C and by resistance to phage lambda. Deletion mutants HD700 (Δ*hyc*), HDK103 (Δ*hya* Δ*hyc*), and HDK203 (Δ*hyb* Δ*hyc*) are derivatives of MC4100 and have been previously described (9). HYD720K (Δ*hyb* Δ*nik*) was constructed by P1 transduction, with HDK203 as the donor strain and HYD720 as the receptor.

Media and growth conditions. Bacteria were routinely grown in Luria-Bertani (LB) medium or on LB plates (18). Anaerobic growth was achieved normally in LBSM medium (LB medium supplemented with 2 μM sodium selenite and 2 μM ammonium molybdate) in 100-ml bottles filled to the top or on LB plates in GasPak anaerobic jars (BBL Microbiology Systems). As required, ampicillin (50 μg/ml) and kanamycin (20 μg/ml) were added. To assess the influence of *groE* mutations and nickel on hydrogenase synthesis, cells were grown at 30°C to early logarithmic growth phase (optical density at 600 nm [OD_{600}] = 0.25), half of the culture was shifted to 43°C to reduce the efficiency of the altered chaperonin proteins in assisting in protein folding, and the other half was kept at 30°C as a control. As noted, 300 μM $NiCl_2$ was added to both 30 and 43°C cultures at the time corresponding to 1 h after the temperature shift. After a 3-h incubation, cells were harvested and broken by two passages through a French press. The enzyme activities and hydrogenase contents in crude extracts were analyzed. Alternatively, 300 μM $NiCl_2$ was added 1 h prior to the temperature shift. Fifty milliliters of culture was removed every hour for measuring the optical density and hydrogenase activity. To prepare an in vitro translation system, *E. coli* MC4100 cells were grown anaerobically at 37°C to mid-logarithmic growth phase in minimal M9 medium (18) supplemented with 10 g of yeast extract per liter and 1% glucose. Cells were harvested, and the crude extract (S-30) and high-speed supernatant (S-135) were prepared as described previously (19).

Intracellular nickel accumulation. Cells were grown in 1 ml of LBSM medium at 30°C to an OD_{600} of 0.25. They were then shifted to 43°C. One hour after the temperature shift, 3.6 μM $^{63}NiCl_2$ plus 300 μM nonradioactive $NiCl_2$, as indicated, was added to the growth medium. Three hours later, 100 μl of culture was removed to measure the OD_{600} and then filtered through cellulose nitrate membrane filters (pore size, 0.45 μm; Whatman). Filters were washed twice with 10 ml of 50 mM Tris-HCl buffer (pH 7.2) containing 10 mM EDTA and transferred to 5 ml of scintillation fluid (OCS; Amersham) for counting with a Kontron SL4000 liquid scintillation counter. Assays were performed in triplicate.

Enzyme assays. To specifically detect HYD1 and HYD2 activities, crude extracts were separated on 7.5% nondenaturing polyacrylamide gels and HYD1 and HYD2 were visualized by a benzyl viologen-linked hydrogen uptake assay (26). The activity bands were fixed by the addition of 1 mM 2,3,5-triphenyltetrazolium chloride. Total hydrogenase activity and nitrate reductase activity were determined as previously described (31). The protein concentration was determined by using a DC protein assay kit (Bio-Rad).

Immunoblot analysis. Denatured polypeptides were separated by SDS-PAGE (11) on 12.5% acrylamide gels. Immunoblotting was performed by the enhanced chemiluminescence method according to the manufacturer's (Amersham) instructions. Antisera were used at the following dilutions: anti-HYD2, 1/10,000; anti-HYD3, 1/5,000 for first probing and 1/2,500 for reprobing; anti-GroEL, 1/10,000 for normal conditions and 1/20,000 for high-stringency conditions; and goat anti-rabbit immunoglobulin G-peroxidase, 1/20,000.

Ligand blotting. Ligand blotting was performed by the method of Soutar and Wade (28). Proteins in crude extracts were separated by SDS-PAGE on 12.5% minigels (7 by 10 cm) run at 200 V. Electrophoresis was stopped 30 min after the dye front had run out of the gel. The remaining proteins with molecular weights higher than 55,000 were electroblotted onto a polyvinylidene difluoride (PVDF) membrane. Membranes were soaked in blocking buffer (20 mM Tris-HCl [pH 7.5], 500 mM NaCl, 3% gelatin) for 1 h, briefly rinsed with two changes of washing buffer (20 mM Tris-HCl [pH 7.5], 500 mM NaCl, 0.1% Tween 20), and washed once for 15 min and twice for 5 min with fresh changes of the washing buffer at room temperature. Membranes were then incubated in in vitro translation buffer (19) containing 40 nM GroES (monomer) and 70 nM GroEL (monomer) with gentle shaking at room temperature for 2 h. Bound GroEL was detected by immunoblotting using anti-GroEL antiserum as described above. GroEL and GroES proteins were purified from an overproducing strain of *E. coli* bearing plasmid pOF39, as described by Ziemienowicz et al. (35).

In vitro synthesis of the large subunit of HYD3 (HycE). A 2.3-kb *Asu*II-*Hin*dIII fragment containing the entire *hycE* gene and a truncated *hycF* gene was subcloned into pT7-5 under the control of the pT7 promoter to give plasmid pMS75 (2). In vitro synthesis of HycE was performed in two steps. Transcription was carried out at 37°C with T7 RNA polymerase and pMS75 as the template according to the manufacturer's (Promega) instructions. The transcription products were added to the in vitro cell-free translation system consisting of the high-speed supernatant (S-135) prepared from anaerobically grown MC4100 (see above). The translation products were labeled with [^{35}S]methionine and [^{35}S]cysteine (NEG-072 EXPRE^{35}S^{35}S; NEN) at 37°C for 30 min as described previously (19). To identify the *hycE* gene product, *hycE* was cleaved at a position corresponding to amino acid position 481 by restriction endonuclease *Eco*RV, leading to the synthesis of a polypeptide that was shorter by 88 C-terminal amino acids. The translation products were precipitated by 5% trichloroacetic acid at 4°C for 30 min. After dissolution in loading buffer (135 mM Tris base, 10 mM EDTA, 3.3% SDS, 11.7% glycerol, 0.012% bromophenol blue, 100 mM dithiothreitol), the samples were separated by SDS-PAGE and visualized by fluorography.

Detection of the HycE-chaperonin complex. As indicated, GroEL 14-mer (0.17 μM) and GroES 7-mer (0.23 μM) or bovine serum albumin (BSA) (0.2 μM) were added to the in vitro transcription-translation system. After 30 min, the translation reaction products were immediately applied onto a 10-ml Sephadex G-150 size exclusion column equilibrated with 50 mM Na_2HPO_4 (pH 7.2)–100 mM NaCl–1 mM dithiothreitol. The column was calibrated with blue dextran 2000 (2,000,000), BSA (68,000), and lysozyme (14,300). Proteins were eluted at 8 ml/h, precipitated with 5% trichloroacetic acid, resolved by SDS-PAGE, and visualized by fluorography.

RESULTS AND DISCUSSION

Effects of *groES* and *groEL* mutations on total hydrogenase activity. To examine the global effect of a chaperonin deficiency on hydrogenase biosynthesis, we first measured total hydrogenase activities in the *groEL673* and *groES619* thermosensitive mutants (Table 1). At 30°C, the *groES* and *groEL* single mutations, carried by strains JZ12 and OFB1111, respectively, resulted in an about 30% reduction in total hydrogenase activity compared with that of the parental wild-type strain B178, indicating that the *groE* mutations affected the biosynthesis of these hydrogenases even at this permissive temperature. When the cultures of *groE* mutants were shifted to a nonpermissive temperature (43°C), hydrogenase activity was reduced to approximately 40% of the wild-type levels under the same conditions. This additional reduction in hydrogenase activity, however, was largely prevented by the addition of nickel to mutant strains (Table 1) (see below).

TABLE 1. Effects of *groES* and *groEL* mutations and nickel on NiFe-hydrogenase activities[a]

Strain	Genotype	Hydrogenase				Nitrate reductase[b]
		−Nickel		+Nickel		
		30°C	30-43°C	30°C	30-43°C	
B178	Wild type	1.35 ± 0.11	1.23 ± 0.12	1.28 ± 0.17	1.16 ± 0.07	0.65
JZ12	*groES*	0.88 ± 0.15	0.48 ± 0.09	0.93 ± 0.10	0.87 ± 0.18	0.60
OFB1111	*groEL*	0.90 ± 0.17	0.45 ± 0.07	0.96 ± 0.15	0.75 ± 0.11	0.54
NB01	*nik*	<0.01	<0.01	0.78 ± 0.15	0.64 ± 0.12	0.69
NB02	*groES nik*	<0.01	<0.01	0.91 ± 0.05	0.22 ± 0.08	0.55
NB03	*groEL nik*	<0.01	<0.01	0.91 ± 0.19	0.07 ± 0.04	0.56

[a] Cells were grown anaerobically in LB medium supplemented with 2 μM sodium selenite and 2 μM ammonium molybdate at 30°C to early-logarithmic-growth phase (OD_{600} = 0.25). Half of the culture was shifted to 43°C (30-43°C) to inactivate the chaperonin proteins, while the other half was kept at 30°C as a control. As noted, 300 μM $NiCl_2$ was added to both 30 and 43°C cultures at the time corresponding to 1 h after the temperature shift. After 3 h of incubation, cells were harvested and broken by two passages through a French press. Hydrogenase and nitrate reductase activities were measured as described in Materials and Methods. Specific activities were defined as 1 μmol of benzyl viologen reduced per min per mg (dry weight) of bacteria for hydrogenase and 1 μmol of nitrate reduced per min per mg (dry weight) of bacteria for nitrate reductase. Data are averages ± standard errors of at least three separate experiments.

[b] Only data from experiments with a temperature shift and in the presence of nickel are reported.

The high temperature (43°C) used to reduce the efficiency of the mutated GroE proteins lies near the upper end of the heat shock range, which can lead to a severe general effect on protein biosynthesis. To address the question of whether the reduction in hydrogenase activity was due to a general failure of protein synthesis and to examine whether *groE* mutations affect anaerobic metalloenzymes in general, we measured the activity of another membrane-bound, oligomeric metalloenzyme, nitrate reductase. There was no significant difference in nitrate reductase activity between the wild type and its *groE* derivatives (Table 1). Therefore, the reduction in the hydrogenase activity of *groES* and *groEL* mutants cannot simply be due to a general secondary effect of *groE* mutations.

Effects of *groES* and *groEL* mutations on HYD1 and HYD2 activities. While these results show a negative effect of *groE* mutations on total hydrogenase activity, they do not indicate to what extent the three isoenzymes were affected individually. Hydrogenase activity staining allowed us to analyze the influences of *groES619* and *groEL673* mutations on HYD1 and HYD2 activities. Crude extracts of different mutants were separated by native PAGE, and the hydrogenase enzymes were visualized by activity staining. Wild-type strain B178 exhibited three active bands (Fig. 1, lane 2), which is in good agreement with the results previously reported by Sawers and Boxer (26). As they demonstrated, the fastest-migrating band corresponds to HYD1 while the two more slowly migrating bands are HYD2. The difference between the two forms of HYD2 is unknown. As anticipated, mutants HDK103 (Δ*hya* Δ*hyc*) and HDK203 (Δ*hyb* Δ*hyc*) display only HYD2 and HYD1 activities, respectively (Fig. 1, lanes 1 and 7). HYD1 activity was absent from both *groES* and *groEL* mutants grown with or without a temperature shift (Fig. 1, lanes 3 to 6). In contrast, HYD2 activity was detected in *groE* mutants at both permissive and nonpermissive temperatures (Fig. 1, lanes 3 to 6), indicating that of these two isoenzymes only HYD1 highly depends on the chaperonin proteins GroEL and GroES. Since this technique is not able to detect HYD3 activity (25), the effects of *groE* mutations on the biosynthesis of HYD3 were studied by an alternative method (see Fig. 4).

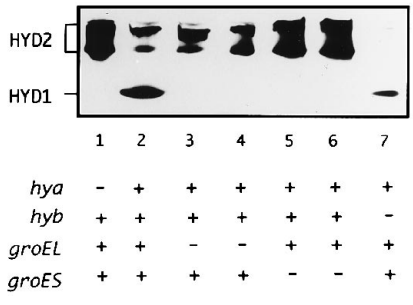

FIG. 1. Effects of *groES* and *groEL* mutations on HYD1 and HYD2 activities. Crude extracts (50 μg of total protein for each sample) of the wild type (lane 2), its *groEL* (lanes 3 and 4) and *groES* (lanes 5 and 6) derivatives, mutant HDK103 (Δ*hya* Δ*hyc*) (lane 1), and mutant HDK203 (Δ*hyb* Δ*hyc*) (lane 7) grown at 43°C (lanes 4 and 6) or 30°C (lanes 1 through 3, 5, and 7) were separated on 7.5% native polyacrylamide gels and stained to reveal hydrogenase activity.

Requirement of chaperonins for hydrogenase biosynthesis at a step prior to nickel incorporation. In order to more closely identify the stages at which chaperonins might be required for the formation of functional hydrogenases, we exploited our *nik* mutant, which allows us to selectively analyze Ni^{2+} incorporation into hydrogenase precursors. The *nik* mutant is defective in its specific nickel transport system, and its intracellular nickel concentration is less than 1% of the level of a wild-type strain, which results in the absence of hydrogenase activity (HYD^- phenotype). The addition of 300 μM nickel to the growth medium restores the intracellular nickel concentration and the hydrogenase activity in this mutant. In this case, nickel is taken up through the nonspecific magnesium transport system (20, 31, 32). Complementation of the HYD^- phenotype of the *nik* mutant by Ni^{2+} could result from (i) an induction of hydrogenase biosynthesis or (ii) the incorporation of nickel into otherwise inactive precursor forms of hydrogenases. To distinguish between these two possibilities, we examined the intracellular levels of hydrogenases by immunoblotting. The identities of the polypeptides recognized by the anti-HYD2 and anti-HYD3 antisera used as the large subunits of HYD2 (HybC) and HYD3 (HycE) were proven by the lack of these bands in mutants HYD720K (Δ*hyb* Δ*nik*) and HD700 (Δ*hyc*), respectively (Fig. 2B and C). Since the purpose of using the double mutant HYD720K (Δ*hyb* Δ*nik*) (Fig. 2B, lane Δ*hyb*) was to verify the identity of HybC, the *nik* mutation here was unimportant. Similar amounts of the large subunits of HYD2 and HYD3 were detected in the wild-type strain and in the *nik* mutant grown in the absence of nickel. Thus, the biosynthesis of HYD2 and HYD3 does not depend on nickel at the transcriptional and translational levels. In the absence of Ni^{2+}, however, both large subunits accumulated as slowly migrating, nonprocessed forms (HybC-P [Fig. 2B, lane *nik* −Ni] and

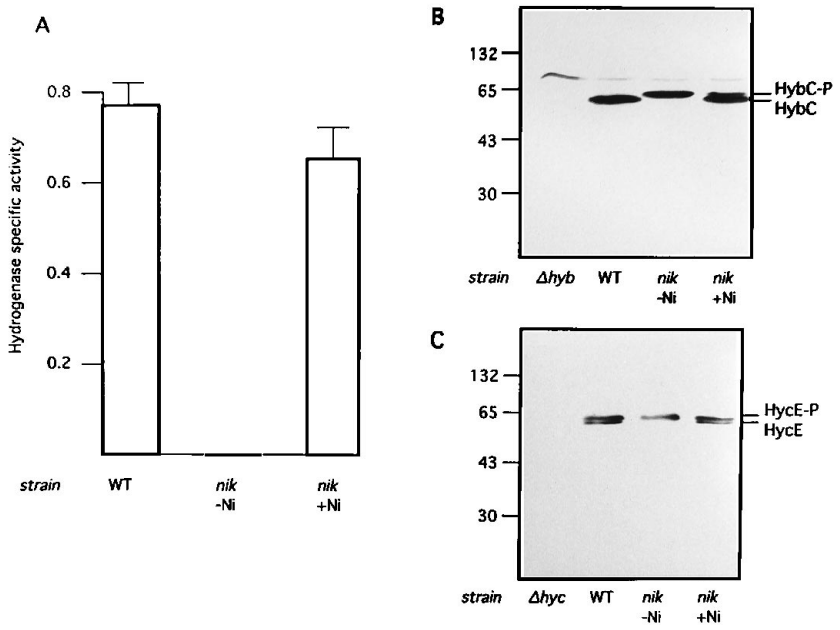

FIG. 2. Nickel-dependent restoration of hydrogenase activity and large subunit processing in the *nik* mutant. Wild-type B178 (WT) and its derivatives NB01 (*nik*), HYD720K (Δ*hyb* Δ*nik*; this strain is described as Δ*hyb* in panel B), and HD700 (Δ*hyc*) were grown anaerobically at 37°C in LB medium. As noted, 300 μM $NiCl_2$ was added to cultures (Δ*nik* + Ni) after 3 h of incubation (OD_{600} = 0.3). After 1 h of additional incubation, cells were harvested. Under these conditions, the processing of the precursor of HybC is not completed, which allows a clear distinction between the precursor and the processed form. For other cultures grown in the absence of nickel (−Ni) (WT, Δ*hyb*, Δ*hyc*, and Δ*nik* Ni), cells were harvested after a total of 4 h of incubation. The hydrogenase specific activity (A) was measured as described in Materials and Methods. The cellular contents of the precursors and processed forms of the large subunits of HYD2 (HybC-P and HybC, respectively) (B) and HYD3 (HycE-P and HycE, respectively) (C) were detected by immunoblotting after the separation of proteins (20 μg for each sample) by SDS–12.5% PAGE. For each culture, the same sample was used to perform the three experiments. Strains HYD720K (Δ*hyb* Δ*nik*) and HD700 (Δ*hyc*) were used here to verify the identities of HybC and HycE, respectively.

HycE-P [Fig. 2C, lane *nik* −Ni]) and hydrogenase activity was undetectable (Fig. 2A, lane *nik* −Ni). The addition of nickel to the growth medium resulted not only in the restoration of hydrogenase activity (Fig. 2A, lane *nik* +Ni) but also in the processing of the large subunits (HybC and HycE [Fig. 2B and C, lanes *nik* +Ni). These results, together with those reported previously (20, 23, 31, 32), suggest that the restoration of hydrogenase activity by nickel in the *nik* mutant likely results from the incorporation of nickel into the precursor, with subsequent processing of the large subunit and activation of the enzymes. It should be noted that both precursor and processed forms of the large subunit of HYD3 were observed in the wild-type strain (Fig. 2C). This may suggest a slow processing procedure for HYD3. The large subunit of HYD1 was also synthesized in the *nik* mutant without nickel (data not shown), but we could not clearly distinguish the precursor from the processed form.

When the *nik* and *groE* mutations were combined, the resultant double mutants showed the anticipated HYD^- phenotype when grown at 30°C without nickel and HYD^+ phenotype after the addition of nickel (Table 1). As shown above for the single *nik* mutants, the large subunits of HYD2 and HYD3 were synthesized in amounts in these double mutants similar to those in the wild-type parental strain (see Fig. 4). However, when nickel was added to the growth medium 1 h after shifting the growth temperature to 43°C, the restoration of hydrogenase activity amounted to only 30% in NB02 (*groES nik*) and 10% in NB03 (*groEL nik*) with respect to that in the single *nik* mutant NB01 or 17 and 5% of that in parental wild-type B178, respectively (Table 1).

The failure of Ni^{2+} to restore the hydrogenase activity in *groE nik* double mutants to the same extent as that seen in either of the single *groE* and *nik* mutants must be the result of the reduced efficiency of the mutated chaperonin in assisting in protein folding preceding the addition of nickel. In theory, it could be caused by impaired intracellular nickel availability after the temperature shift. This possibility, however, was excluded by the finding that the amount of ^{63}Ni accumulating in the wild-type parental strain is comparable to that in the *groE* mutants. Wild-type strain B178 was found to contain 3.4 and 0.6 nmol of nickel per mg (dry weight) of bacteria in cells grown without and with 300 μM nonradioactive nickel, respectively. The corresponding values for the *groES* mutant were 4.2 and 0.7 nmol of nickel per mg (dry weight) of bacteria, and those for the *groEL* mutant were 3.7 and 0.6 nmol of nickel per mg (dry weight) of bacteria. Therefore, the accumulation of intracellular nickel via the specific or nonspecific nickel uptake system does not seem to be affected by *groE* mutations.

The inability of Ni^{2+} to restore hydrogenase activity after the temperature shift in a *nik* background would also be expected to occur if the chaperonins were involved in a step preceding nickel incorporation into the precursor during the biosynthesis of hydrogenases. To assess this point, nickel was added to the growth medium prior to the temperature shift to allow for the normal incorporation of nickel into the hydrogenase precursors in *nik groE* mutants in the presence of active chaperonins. One hour after the addition of nickel, cultures were shifted to 43°C for 3 additional h to reduce the efficiency of mutated chaperonins in assisting in protein folding, while the controls were kept at 30°C. Half an hour after the temperature shift, the growth rates of cultures at 43°C started to lag behind those of cultures at 30°C (data not shown), indicating the effects of reduced chaperonin efficiency. Hydrogenase activity increased steadily over this period of growth, regardless

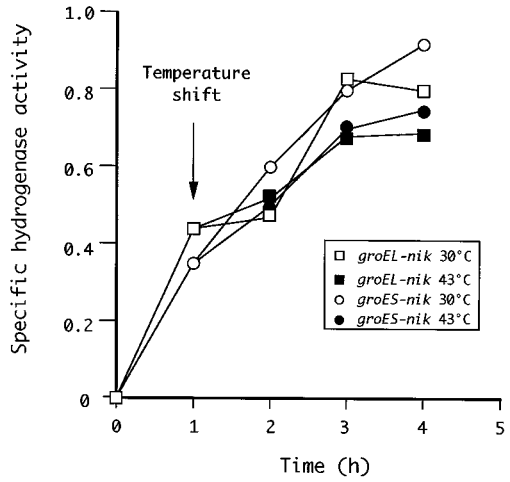

FIG. 3. Effects of chaperonin deficiency on the restoration of hydrogenase activity. $NiCl_2$ (300 μM) was added to the growth medium at 30°C when the OD_{600} of cultures was 0.25 (corresponding to zero time). One hour later, half of the culture was shifted to 43°C to reduce mutated chaperonin efficiency, whereas the other half of the culture was kept at 30°C. Cells were harvested, and hydrogenase activity was measured as described in Materials and Methods.

of whether or not cultures were subjected to heat shock (Fig. 3). It was repeatedly observed that 3 h after the temperature shift, the specific hydrogenase activity of cultures at 43°C remained approximately 80% of that of controls kept at 30°C. Therefore, in Ni^{2+}-depleted cells, the reduction in the efficiency of altered chaperonins in assisting in protein folding by temperature shift markedly inhibits the nickel-mediated restoration of hydrogenase activity only if it precedes the addition of nickel.

Effects of *groES* and *groEL* mutations on the processing of the large subunits of HYD2 (HybC) and HYD3 (HycE). As depicted in Fig. 2, hydrogenases are synthesized at normal levels in the *nik* mutant in the absence of nickel. However, they are not active and the large subunits accumulate in nonprocessed forms. The addition of nickel to the growth medium leads to the processing of the large subunits and the restoration of hydrogenase activity. To show directly the involvement of chaperonin proteins in nickel-dependent processing of the large subunits of HYD2 (HybC) and HYD3 (HycE), immunoblot experiments subsequent to the separation of proteins of a crude extract by SDS-PAGE were performed (Fig. 4).

Only the faster-migrating processed form of the large subunit of HYD2 (HybC) was detected in the wild-type strain and *groE* single mutants (Fig. 4A, lanes 1 to 5 [cf. Fig. 2B lane WT]) under most of the conditions used, which is consistent with the unimpaired HYD2 activity demonstrated in Fig. 2. On the contrary, only the precursor form of the large subunit of HYD2 was detected in *groE nik* mutants in the absence of nickel (Fig. 4A, lanes 6 to 10). Similar to the situation with the *nik* mutant (Fig. 4A, lane 6), the addition of nickel led to complete processing of the large subunit of HYD2 in *groES nik* mutants at both 30 and 43°C (Fig. 4A, lanes 6 to 8). In the *groEL nik* mutant, however, Ni^{2+} fully overcame the *nik*-mutant-specific defect in processing only at the permissive temperature (Fig. 4A, lane 9), whereas the temperature shift led to some residual precursor of the large subunit of HYD2 (Fig. 4A, lane 10). Thus, processing of the large subunit of HYD2 was independent of GroES activity and largely independent of GroEL activity.

In contrast to HYD2, however, the large subunit of HYD3 (HycE) was found exclusively in its nonprocessed precursor form in all *groE* derivatives in the absence of nickel (Fig. 4B, lanes 2 to 10). Even in wild-type strain B178, only partial processing of this subunit was observed upon heat treatment (Fig. 4B, lane 1). The addition of nickel to *nik groE* derivatives led to only a small relief of the block in precursor processing when cells were grown at the permissive temperature, i.e., in the presence of at least partially functional chaperonins (Fig. 4B, lanes 7 and 9). However, this inefficient processing of the large subunit of HYD3 (HycE) was completely abolished when the mutant chaperonins were subjected to heat shock treatment (Fig. 4B, lanes 8 and 10). These results clearly demonstrate that the precursor of the large subunit of HYD3 requires active chaperonins for processing.

The data described so far demonstrate an involvement of GroES and GroEL in the biosynthesis of HYD1 and HYD3, while HYD2 was found to be largely independent of chaperonins. This is consistent with the report by Sawers and coworkers that HYD1 represents less than 10% of total activity under all conditions, whereas HYD3 constitutes a major portion of the total activity, ranging from 40 to 95% depending on the growth medium used (25). Therefore, HYD2 may account for the remainder of the hydrogenase activity in *nik groE* double mutants (Table 1). The $HYD1^-$ phenotype of the *groEL* and *groES* mutants might be due to a failure to be translated, to proteolytic degradation, or to an aggregation after synthesis in the absence of chaperonins. The lack of anti-HYD1 antiserum of sufficiently high quality prevented us from carrying out further studies, such as those performed with HYD2 and HYD3.

The differences in the dependence of the two isoenzymes HYD2 and HYD3 on chaperonins might be determined by their different cellular locations. HYD2 is an integral membrane protein with a probable bitopic structure, because it can be solubilized in an active form after treatment of the membrane fraction with trypsin (25). The observation that HYD2 becomes accessible in spheroplasts (21a) suggests that a large part of it must be located on the periplasmic side. A trans-

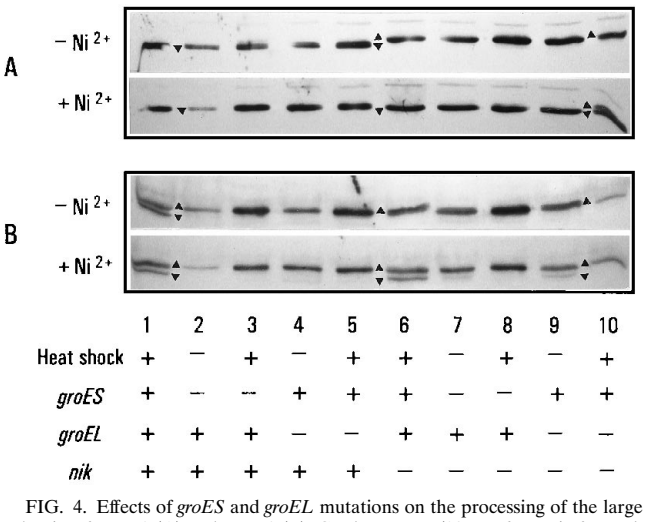

FIG. 4. Effects of *groES* and *groEL* mutations on the processing of the large subunits of HYD2 (A) and HYD3 (B). Crude extracts (20 μg of protein for each sample) of the wild type (lane 1) and its *groES* (lanes 2 and 3), *groEL* (lanes 4 and 5), *nik* (lane 6), *groES nik* (lanes 7 and 8), and *groEL nik* (lanes 9 and 10) derivatives were separated by SDS–12.5% PAGE and electrotransferred to a membrane. HybC (A) and HycE (B) were detected by immunoblotting. The application (+) or not (−) of a temperature shift to early-logarithmic-growth cultures 1 h prior to the time corresponding to when 300 μM nickel was added is indicated. Precursor and processed forms of HybC and HycE are indicated by triangles pointing upwards and downwards, respectively.

membrane translocation process possibly involving the Sec proteins is thus required for HYD2 biosynthesis. HYD3 is a peripheral membrane protein, located on the cytoplasmic side, and is released into the soluble state when cells are broken by passage through a French press (24). The differential dependence of HYD2 and HYD3 biosynthesis on chaperonins is thus in agreement with the conclusion of Horwich et al. that only a specific set of cytoplasmic proteins depends on GroEL function, whereas the class of exported proteins does not seem to require GroEL function stringently (8).

Binding of chaperonins to the precursor of the large subunit of HYD3 (HycE). The data presented so far are consistent with the following scenario: a reduction in the efficiency of altered chaperonins GroEL and GroES in assisting in protein folding causes the large subunit of HYD3 to accumulate as an unprocessed precursor (Fig. 4). This is paralleled by a drastic drop in total hydrogenase activity (Table 1). Processing of the HYD3 precursor requires the presence of Ni^{2+}, as demonstrated by use of the *nik* mutant (Fig. 2C). Since we can rule out intracellular deprivation of Ni^{2+} after the decrease in active chaperonins, the lack of functional GroE proteins must prevent the precursor from reaching a conformation competent for the incorporation of nickel. If GroE proteins improve the efficiency of the incorporation of Ni^{2+} into the precursor of the large subunit of HYD3, one would expect that a GroE deficiency could be partially compensated for by exogenously added Ni^{2+}. This is exactly what we observed (Table 1).

We next attempted to directly demonstrate the binding of the large subunit of HYD3 to GroEL by size exclusion chromatography and ligand blotting. HycE was synthesized by a cell-free transcription-translation system prepared from anaerobically grown wild-type *E. coli* MC4100 and programmed with plasmid pMS75. A major translation product with a molecular mass of approximately 64 kDa was thus obtained (Fig. 5A and B, lanes P), which is in agreement with that of purified HycE (2). The fact that this protein is indeed the translation product of the *hycE* gene was indicated by the synthesis of a smaller polypeptide when pMS75 had been cleaved within the *hycE* gene by restriction endonuclease *Eco*RV (data not shown). After in vitro synthesis in the presence or absence of chaperonins in the reaction medium, radiolabeled HycE was immediately analyzed by size exclusion chromatography. The Sephadex G-150 matrix (Pharmacia) used in this study has a fractionation range for globular molecules with molecular masses between 5×10^3 and 3×10^5 Da. The column was calibrated with blue dextran 2000 (2,000,000), BSA (68,000), and lysozyme (14,300). The elution of blue dextran peaked in fraction 22 and ended at fraction 27. BSA eluted in fractions 33 to 44. Since GroEL forms complexes composed of 14 monomers of GroEL (M_r = 57,259) (7), this material with a molecular mass of about 800,000 Da should be excluded from the beads of the matrix and pass through the column within the exclusion volume. Fractions collected from the column were loaded on SDS-PAGE gels for analyzing the components. In the absence of chaperonin proteins, ^{35}S-labeled HycE was located in fractions 33 to 44 (Fig. 5A). When chaperonin proteins were added to the in vitro translation reaction mixture, HycE was also detected in fraction 22 and significantly more of it was recovered from fractions 27 and 33 when compared with the corresponding fractions of the chaperonin-free control (compare Fig. 5B and A). Therefore, a HycE-chaperonin complex seems to have formed in vitro under these conditions and consequently was excluded from the pore matrix.

The binding of GroEL to HycE was further examined by ligand blotting. Proteins in crude extracts were separated by SDS-PAGE. Because electrophoresis was stopped half an hour after the dye front had run out of the gel, only polypeptide chains with molecular weights higher than 55,000 were retained on the gel. These were then electroblotted onto a PVDF membrane. When the membrane was probed with anti-GroEL or anti-HycE antiserum, only GroEL or HycE was detected, respectively (Fig. 5C, lanes 2, 8, and 9), indicating specificity of these antisera. To analyze the binding of chaperonins to immobilized proteins, first the PVDF membrane was incubated with chaperonins, and then bound GroEL as well as the endogenous GroEL of crude extracts was detected with anti-GroEL antiserum. Under low-stringency conditions, GroEL

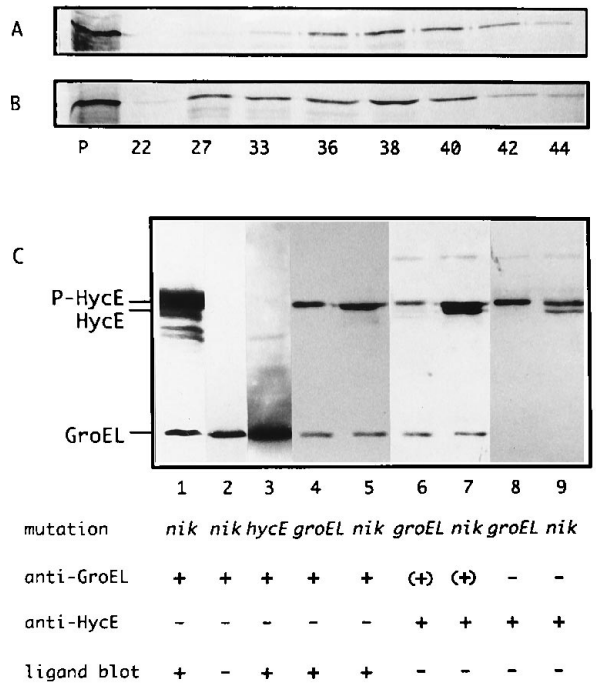

FIG. 5. Binding of the large subunit of HYD3 (HycE) by chaperonins. The large subunit of HYD3 (HycE) was synthesized in vitro by a cell-free transcription-translation system prepared from anaerobically grown *E. coli* MC4100 and programmed with plasmid pMS75 in the presence of BSA (A) or chaperonin proteins (B). The total amount of [^{35}S]methionine- and [^{35}S]cysteine-labeled translation products was immediately applied onto a 10-ml Sephadex G-150 size exclusion column equilibrated with 50 mM Na_2HPO_4 (pH 7.2)–100 mM NaCl–1 mM dithiothreitol. Proteins were eluted, precipitated with 5% trichloroacetic acid, resolved by SDS-PAGE, and visualized by fluorography. The numbers below the lanes in panels A and B are the elution fraction numbers; lanes P, the corresponding translation products prior to chromatography. (C) Crude extracts (20 μg of protein for each sample) of OFB1111 (*groEL*) (lanes 4, 6, and 8), NB01 (*nik*) (lanes 1, 2, 5, 7, and 9), and HD700 (lane 3) grown with 300 μM nickel and subjected to heat treatment were separated by SDS–12.5% PAGE and electroblotted onto a PVDF membrane. In ligand blotting experiments, immunodetection was performed either directly with anti-GroEL (lane 2) or anti-HycE (lanes 8 and 9) antiserum or after incubation of the membrane with chaperonins and with anti-GroEL antiserum under low-stringency conditions (1/10,000 dilution, 10- to 20-min exposure) (lanes 1 and 3) or high-stringency conditions (1/20,000 dilution, 1- to 5-min exposure) (lanes 4 and 5). The same membrane shown in lanes 4 and 5 was reprobed by anti-HycE antiserum (lanes 6 and 7). The appearance of the processed-HycE band only after reprobing with anti-HycE antiserum (lane 7) shows that the HycE signals in lanes 6 and 7 indeed must reflect HycE-cross-reactive material. They are therefore not simply carried over from the previous probing with anti-GroEL antiserum, as could have been inferred from the fact that the GroEL band remained visible in lanes 6 and 7 after the reprobing procedure, whereas it did not light up when the blot was developed with anti-HycE antiserum only (lanes 8 and 9). The positions of the precursor (P-HycE) and processed (HycE) forms of the HYD3 large subunit and GroEL are on the left. The use (+) or not (−) of the corresponding antiserum or a ligand blotting procedure is indicated. Parentheses indicate that the same membrane was reprobed with anti-HycE antiserum after ligand blotting.

was found associated with few immobilized proteins (Fig. 5C, lane 1). Only one of these polypeptides was also detected under high-stringency conditions, i.e., with a higher dilution of anti-GroEL antiserum and a shorter exposure time (Fig. 5C, lanes 4 and 5). Thus, the detection of this polypeptide with GroEL seems more sensitive or efficient than with others under the conditions used. This band must result from the binding of GroEL to HycE, since it was absent from an extract of HD700, which bears a deletion of the entire *hyc* operon (Fig. 5C, lane 3). Moreover, a slightly smaller, additional band became visible in an extract of NB01 (*nik*) grown with nickel when after ligand blotting, the same membrane (Fig. 5C, lanes 4 and 5) was reprobed with anti-HycE antiserum (lane 7). This additionally detected band was superimposable with the processed form of HycE (Fig. 5C; compare lane 7 with lane 9). As such, it was absent from extracts of OFB1111 (*groEL*) after heat treatment (Fig. 5C; compare lane 7 with lane 6), which correlates with the finding described above that the processed form of HycE was present in the *nik* mutant grown with nickel but absent in the *groEL* mutant grown at the nonpermissive temperature (Fig. 5B, lanes 5 and 6). This correlation also holds true for the wild-type strain and *groES* derivatives (data not shown). Thus, ligand blotting using GroEL not only demonstrated the binding of GroEL to HycE but also suggested a certain specificity of the process in that GroEL was found to bind only to the precursor of HycE. Altogether, the results presented in Fig. 5 strongly support our results obtained in vivo, i.e., a clear-cut requirement for GroEL in the processing of HycE.

Recently, the crystal structure of the NiFe-hydrogenase from *D. gigas* was solved at 2.85-Å (1 Å = 0.1 nm) resolution (29). The active site containing nickel and a second metal ion, probably an iron, is deeply buried in the 60-kDa large subunit. The structural data also reveal that the last 15 C-terminal residues deduced from the gene sequence are absent, indicating a cleavage occurring just after the histidinyl residue in the DPCXXCXXH motif conserved in all nickel-containing hydrogenases. Studies performed by Rossmann and coworkers showed that the removal of the corresponding extra C-terminal segment of the large subunit of HYD3 (HycE) was catalyzed by a specific protease and was correlated with the incorporation of nickel into the precursor (22, 23). Therefore, the DPCXXC XXH motif, of which the two cysteinyl residues serve as bridging ligands of the two metal ions in the active center, and the extra C-terminal segment must be located on the surface of the precursor of the large subunit. The incorporation of nickel and the second ion into the active center triggers conformational change and the removal of the extra C-terminal segment, which are followed by the formation of the active site deeply buried in the mature enzyme. Removal of the extra C-terminal segment makes these processes irreversible. As a new aspect to this scenario, we add here the involvement of chaperonins in assisting the HycE precursor to reach a conformation competent for the insertion of nickel.

Our future studies will focus on characterization of the nickel incorporation mechanism, on the influence of chaperone proteins on nickel-dependent assembly, on translocation of hydrogenases, and on the identification of putative chaperones specific for hydrogenase isoenzymes.

ACKNOWLEDGMENTS

We acknowledge A. Böck for critically reading the manuscript and for valuable suggestions. We thank T. Langer for valuable discussions concerning chaperonin binding and its effect on cytoplasmic protein biosynthesis. We also thank D. H. Boxer for the generous gift of anti-HYD2 antiserum, W. Nasser for advice regarding size exclusion chromatography, K. de Pina for helpful discussions, and A. de Christene for help with the artwork.

This work was supported by grants from the Centre National de la Recherche Scientifique to UMR CNRS 5577 and UPR CNRS 9007, from the Association pour la Recherche sur le Cancer (grant 2067 to O.F.), from the Sonderforschungsbereich 184 and the Fonds der Chemischen Industrie (to M.M.), and from the program PROCOPE (to L.-F.W. and M.M.). L.-F.W. acknowledges the European Molecular Biology Organization (EMBO) for a short-term fellowship award and the generous hospitality of Institut für Physikalische Biochemie, Universität München, which made this study possible.

REFERENCES

1. **Ballantine, S. P., and D. H. Boxer.** 1986. Isolation and characterisation of a soluble active fragment of hydrogenase isoenzyme 2 from the membranes of anaerobically grown *Escherichia coli*. Eur. J. Biochem. **156:**277–284.
2. **Böhm, R., M. Sauter, and A. Böck.** 1990. Nucleotide sequence and expression of an operon in *Escherichia coli* coding for formate hydrogenlyase components. Mol. Microbiol. **4:**231–243.
3. **Braig, K., Z. Otwinowski, R. Hegde, D. C. Boisvert, A. Joachimiak, A. L. Horwich, and P. B. Sigler.** 1994. The crystal structure of the bacterial chaperonin GroEL at 2.8 Å. Nature (London) **371:**578–586.
4. **Friedrich, C. G., K. Schneider, and B. Friedrich.** 1982. Nickel in the catalytically active hydrogenase of *Alcaligenes eutrophus*. J. Bacteriol. **152:**42–48.
5. **Georgopoulos, C. P., R. W. Hendrix, S. R. Casjens, and A. D. Kaiser.** 1973. Host participation in bacteriophage lambda head assembly. J. Mol. Biol. **76:**45–60.
6. **Gollin, D. J., L. E. Mortenson, and R. L. Robson.** 1992. Carboxyl-terminal processing may be essential for production of active NiFe hydrogenase in *Azotobacter vinelandii*. FEBS Lett. **309:**371–375.
7. **Hemmingsen, S., C. Woolford, S. van der Vies, K. Tilly, D. Denis, C. Georgoloulos, R. Hendrick, and R. Ellis.** 1988. Homologous plant and bacterial proteins chaperone oligomeric protein assembly. Nature (London) **333:**330–334.
8. **Horwich, A. L., K. B. Low, W. A. Fenton, I. N. Hirshfield, and K. Furtak.** 1993. Folding in vivo of bacterial cytoplasmic proteins: role of GroEL. Cell **74:**909–917.
9. **Jacobi, A., R. Rossmann, and A. Böck.** 1992. The *hyp* operon gene products are required for the maturation of catalytically active hydrogenase isoenzymes in *E. coli*. Arch. Microbiol. **158:**444–451.
10. **Kortlüke, C., and B. Friedrich.** 1992. Maturation of the membrane-bound hydrogenase of *Alcaligenes eutrophus* H16. J. Bacteriol. **174:**6290–6293.
11. **Laemmli, U. K.** 1970. Cleavage of structural proteins during the assembly of the head of bacteriophage T4. Nature (London) **227:**680–685.
12. **Landry, S. J., J. Zeilstra-Ryalls, O. Fayet, C. Georgopoulos, and L. M. Glerasch.** 1993. Characterization of a functionally important mobile domain of GroES. Nature (London) **364:**255–258.
13. **Lutz, S., A. Jacobi, V. Schlensog, R. Böhm, G. Sawers, and A. Böck.** 1991. Molecular characterization of an operon (*hyp*) necessary for the activity of the three hydrogenase isoenzymes in *Escherichia coli*. Mol. Microbiol. **5:**123–135.
14. **Menon, A. L., and R. L. Robson.** 1994. In vivo and in vitro nickel-dependent processing of the [NiFe] hydrogenase in *Azotobacter vinelandii*. J. Bacteriol. **176:**291–295.
15. **Menon, N. K., C. Y. Chatelus, M. Dervartanian, J. C. Wendt, K. T. Shanmugam, H. D. Peck, Jr., and A. E. Przybyla.** 1994. Cloning, sequencing, and mutational analysis of the *hyb* operon encoding *Escherichia coli* hydrogenase 2. J. Bacteriol. **176:**4416–4423.
16. **Menon, N. K., J. Robbins, H. D. Peck, Jr., C. Y. Chatelus, E.-S. Choi, and A. E. Przybyla.** 1990. Cloning and sequencing a putative *Escherichia coli* [NiFe] hydrogenase-1 operon containing six open reading frames. J. Bacteriol. **172:**1969–1977.
17. **Menon, N. K., J. Robbins, J. C. Wendt, K. T. Shanmugam, and A. E. Przybyla.** 1991. Mutational analysis and characterization of the *Escherichia coli hya* operon, which encodes [NiFe] hydrogenase 1. J. Bacteriol. **173:**4851–4861.
18. **Miller, J. H.** 1972. Experiments in molecular genetics. Cold Spring Harbor Laboratory, Cold Spring Harbor, N.Y.
19. **Müller, M., and G. Blobel.** 1984. In vitro translocation of bacterial proteins across the plasma membrane of *Escherichia coli*. Proc. Natl. Acad. Sci. USA **81:**7421–7425.
20. **Navarro, C., L.-F. Wu, and M. A. Mandrand-Berthelot.** 1993. The *nik* operon of *Escherichia coli* encodes a periplasmic binding protein-dependent transport system for nickel homologous to the peptide permease family. Mol. Microbiol. **9:**1181–1191.
21. **Przybyla, A. E., J. Robbins, N. Menon, and H. D. Peck, Jr.** 1992. Structure-function relationships among the nickel-containing hydrogenases. FEMS Microbiol. Rev. **88:**109–136.

21a. **Rodrigue, A., et al.** Unpublished data.

22. **Rossmann, R., T. Maier, F. Lottspeich, and A. Böck.** 1995. Characterisation

of a protease from *Escherichia coli* involved in hydrogenase maturation. Eur. J. Biochem. **227:**545–550.
23. **Rossmann, R., M. Sauter, F. Lottspeich, and A. Böck.** 1994. Maturation of the large subunit (HYCE) of *Escherichia coli* hydrogenase 3 requires nickel incorporation followed by C-terminal processing at Arg537. Eur. J. Biochem. **220:**377–384.
24. **Sauter, M., R. Böhm, and A. Böck.** 1992. Mutational analysis of the operon (*hyc*) determining hydrogenase 3 formation in *Escherichia coli*. Mol. Microbiol. **6:**1523–1532.
25. **Sawers, R. G., S. P. Ballantine, and D. H. Boxer.** 1985. Differential expression of hydrogenase isoenzymes in *Escherichia coli* K-12: evidence for a third isoenzyme. J. Bacteriol. **164:**1324–1331.
26. **Sawers, R. G., and D. H. Boxer.** 1986. Purification and properties of membrane-bound hydrogenase isoenzyme 1 from anaerobically grown *Escherichia coli* K-12. Eur. J. Biochem. **156:**265–275.
27. **Sorgenfrei, O., D. Linder, M. Karas, and A. Klein.** 1993. A novel very small subunit of a selenium containing [NiFe] hydrogenase of *Methanococcus voltae* is posttranslationally processed by cleavage at a defined position. Eur. J. Biochem. **213:**1355–1358.
28. **Soutar, A. K., and D. P. Wade.** 1990. Ligand blotting, p. 55–76. *In* T. E. Creighton (ed.), Protein function: a practical approach. IRL Press, Oxford.
29. **Volbeda, A., M.-H. Charon, C. Piras, E. C. Hatchikian, M. Frey, and J. C. Fontecilla-Camps.** 1995. Crystal structure of the nickel-iron hydrogenase from *Desulfovibrio gigas*. Nature (London) **373:**580–587.
30. **Wu, L.-F., and M. A. Mandrand.** 1993. Microbial hydrogenases: primary structure, classification, signatures and phylogeny. FEMS Microbiol. Rev. **104:**243–270.
31. **Wu, L.-F., and M. A. Mandrand-Berthelot.** 1986. Genetic and physiological characterisation of new *Escherichia coli* mutants impaired in hydrogenase activity. Biochimie (Paris) **68:**167–179.
32. **Wu, L.-F., M. A. Mandrand-Berthelot, R. Waugh, C. J. Edmont, S. E. Holt, and D. H. Boxer.** 1989. Nickel deficiency gives rise to the defective hydrogenase phenotype of *hydC* and *fnr* mutants in *Escherichia coli*. Mol. Microbiol. **3:**1709–1718.
33. **Wu, L.-F., C. Navarro, and M. A. Mandrand-Berthelot.** 1991. *hydC* region contains a multicistronic operon (*nik*) involved in nickel metabolism in *Escherichia coli*. Gene **107:**37–42.
34. **Zeilstra-Ryalls, J., O. Fayet, L. Baird, and C. Georgopoulos.** 1993. Sequence analysis and phenotypic characterization of *groEL* mutations that block λ and T4 bacteriophage growth. J. Bacteriol. **175:**1134–1143.
35. **Ziemienowicz, A., D. Skowyra, J. Zeilstra-Ryalls, O. Fayet, C. Georgopoulos, and M. Zylicz.** 1993. Both the *Escherichia coli* chaperone systems, GroEL/GroES and DnaK/DnaJ/GrpE, can reactivate heat-treated RNA polymerase. Different mechanisms for the same activity. J. Biol. Chem. **268:**25425–25431.